Comparison of 2D and 3D Angled Samples in High Speed Wind Tunnel

Ben Rasmussen
Department of Physics and Astronomy, University of Victoria
(Dated: March 15, 2024)

The behaviour of mach angles in a high speed wind tunnel was investigated for two geometrically distinct impact targets. The first sample used was a wedge mounted to the end of the tunnel with an impact angle of $8^o \pm 0.5^o$. The second sample was a cone, machined to mirror the same impact angle as the wedge. The samples were subjected to a significant pressure difference inside of the tunnel, allowing for supersonic air flow to occur. This flow generated supersonic Mach angles incident on the samples. The angle of these regions of air lead to the determination of the Mach number in the chamber for increasing values of the pressure gradient on both samples which were fitted linearly to show the relation between pressure and mach number as well as the differences between the cone and wedge. The largest values of the mach number were found to be $M^w_{max} = 1.074$ and $M^c_{max} = 1.066$ at a pressure of 84 psi. The calibration linear relations were found to be $M(P)_{wedge} = (2.9 \pm 0.6) \cdot 10^{-4} \frac{1}{psi}\ P + (1.04 \pm 0.003)$ for the wedge sample and $M(P)_{cone} = (1.0 \pm 0.7) \cdot 10^{-4} \frac{1}{psi}\ P + (1.05 \pm 0.005$ for the cone. Apart from the quantitative difference in the calculated mach numbers, it was found that the wedge sample demonstrated much stronger shocks due in part to the oblique nature of the component with respect to the shocks of the cone. Due to uncertainty in the experiment, these fits are only tentative calibration at best but the relationship was demonstrated nonetheless. future work may be able to obtain a more robust model for the behaviour of the shocks on these particular samples in the high speed wind tunnel.

I. INTRODUCTION

When air within confined spaces is subject to significant gradients in pressure, flow within this region may reach speeds that are supersonic with respect to the speed on sound in the medium. When objects are placed in the path of this flow, the response of the system is dependent on both the speed of the flow and the morphology of the incident face of the object. Generally speaking, the velocity field of a fluid will follow continuous streamlines when in transit and so when incident on a surface with sharp angles, this flow will adjust to pass the object depending on its speed relative to the local speed of sound. In subsonic flow regimes, the flow will likely be of a laminar nature and pass over the object. If the pressure gradient is sufficiently large, such that there exists supersonic flow within the region, the streamlines experience abrupt changes in direction. This is due to the fact that the influence of fluid elements in the medium can only propagate with the intrinsic speed of sound in the fluid and so supersonic flow leads to a disruption in the so-called back propagation of the upstream vector field. When this condition is achieved, the state of the flow around the object generates a shockwave.

Shockwaves come up in many different scientific and engineering phenomena. In this experiment, the behaviour of shockwaves around two different metal obstructions in the flow are analyzed both qualitatively and quantitatively. In a very approximate sense the wedge angle used emulates the front facing angle of a wing with respect to fluid flow while the cone angle used matches the expected behaviour of the front of a jet or space shuttle.

Theory:

Theory Of Mach Angles

For supersonic flows, oblique angles present within the path will generate shockwaves. These shockwaves can be characterized by the angle with which they are deflected with respect to the object in the path. The details of these angles are generally quite complex, depending on the pressure gradient, temperature of the air and the angle of the obstruction tangential to the fluid flow. If the angle of the shockwave, called the mach angle, is much greater than the angle of the object, we may describe the flow in the chamber by the mach number, of the ratio of the fluid speed with the local speed of sound. This approximate relation is given by:

$$\mu = arcsin\left(\frac{1}{M}\right) \tag{1}$$

Where μ is the angle of the shock and M is the

mach number. This equation is derived using the relative passage of Rearranging and solving for the mach number in terms of the mach angle we arrive at:

$$M = \frac{1}{sin\mu} \tag{2}$$

Now this is not strictly accurate for changes in the front of the face of the obstruction but can be used as a method to estimate the speed of the flow around the object. Much more detailed calculations could be completed that include the other parameters of the system given adequate time.

II. METHOD

Imaging the Shock

To perform this experiment, a the internals of a high speed wind tunnel was imaged using a Schlieren imaging set up. The apparatus consisted of a high pressure tank that could be filled with the line pressure that is run throughout the Elliott building. This tank was connected to a chamber that terminated with a Laval nozzle that focused the stream of air onto our samples. This is the point where the samples were mounted. To image the response of the system to a high pressure gradient and super sonic flow, Schlieren imaging was used. This type of imaging allows for the visualization of density variations within an otherwise transparent medium by leveraging the refraction of light through different regions of the fluid. The refractive index of air depends on the density of the air, and as such, when flow disrupts the homogeneity of the local density, light traveling through it experiences different levels of refraction. We may then image shockwaves that cause density variations by using this technique.

The Schlieren apparatus consisted of a number of components on an optics table. Light from a flashlight was focussed into a beam splitter. This light passed through a variable aperture into a collimator beam focused on the target. This light was reflected back from behind the sample, back into the collimator and aperture and was finally split back into a camera with another lens places in front for focus.

Impact Samples Used

Two distinct components were used to compare the difference between the behaviour of the shock angles. The motivation here was to explore how comparable geometric angles of a sample were influenced by changes in the head on shape of the structure. The first sample used can be seen in 1. It was a simple wedge with an angle along two of the axes such that the flow of air formed an oblique shock along this edge.

FIG. 1: Front and side images of the *wedge* impact sample used. The angle of the sample was measured to be $8^0 \pm 0.1^0$. Mounts are present at the bottom so as to connect it properly inside of the Laval nozzle chamber.

The other sample used was a cone of comparable angle to that of the wedge with similar angle length. This can be seen in Fig. 2. The cone emulates the same angle and side length but with a continuous angular front face. This means that the created shock angle will likely be radially symmetric about the tip of the cone.

Taking Data

To take data, the high pressure tank was filled to the desired pressure using the main-line in the Elliott building. The valve controlling this was then swiftly opened while the camera recorded the samples. The

FIG. 2: Front and side images of the *cone* impact sample used. The sample was machined so as to emulate the same angle as the wedge, which is roughly $8^0 \pm 0.1^0$. Mounts are once against present to connect to the Laval nozzle chamber. Chutes have been made to either side of the sample to allow for airflow.

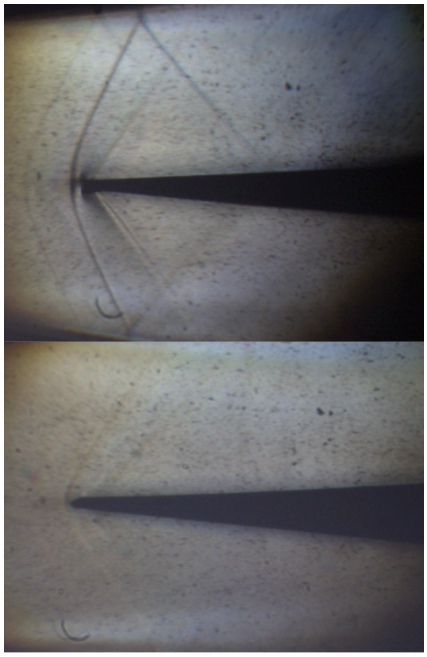

FIG. 3: Images of shockwaves produced from an applied pressure of 89 ± 0.5 psi for both the wedge and cone sample. Shock is much more pronounced for the wedge sample compared to the cone due in part to the Schlieren set up between the two data runs.

videos were then analyzed such that a single frame was selected with the produced shockwave reaching a steady state over a number of frames. This was then repeated from the maximum pressure capable due to the line pressure, down to the lowest possible pressure that still produced a shock in increments of 5 psi. The value where a shock was still produced differed significantly between the samples.

The result of a run on both the cone and wedge sample can be seen in Fig. 3. These are both for the maximum possible pressure, with the two samples showing significantly different magnitudes of shock. This will be explained later, but it is likely that the efficacy of the Schlieren imaging for the cone was reduced when compared to the wedge.

Refining Results:

To find the values of the mach number for a specific pressure and sample used, a number of steps were taken. As seen in Fig. 3, the schlieren imaging allows for well resolved shockwaves to be captured. These images were put into LoggerPro and the path of the shockwave with respect to the wedge or cone was traced, recording pixel data point pairs. The violent nature of an individual data run caused the entire imaging system to be shaken, causing both the position and the angle of the camera to change run-to-run. This was mitigated by re-centering the front of the shockwave to the point where they began, essentially moving the front of the shock to the same pixel position for all pressure runs. After re-centering, the angle of the shock was obtained by continuing the linear regime of the shock to a point in front of the shock angle and applying the following formula:

$$\theta = arctan\left(\frac{y_{pix}}{x_{pix}}\right) \tag{3}$$

With an angle of the shock obtained for both samples and each pressure increment obtained, it was possible to obtain approximate values of the mach number present within the tube using equation (1).

These values for both the cone and the wedge were fit with a simple linear relation to calibrate the speed in the tube with differing results.

III. RESULTS AND ANALYSIS

The traces of each shock wave can be seen in Fig. 4 for the wedge sample. The increasing colour corresponds to an increasing applied pressure to the system. We can see that there is a relationship between angle and the pressure from the tank, but that it is clearly not monotonic. This is largely due to a significant amount of uncertainty in the system that will be discussed later. Two inhibitors of quality data obtained can be attributed to the movement of the camera during each run caused by the shaking of the underlying table and the difficulty (especially for the cone) of tracing the curve of the shock.

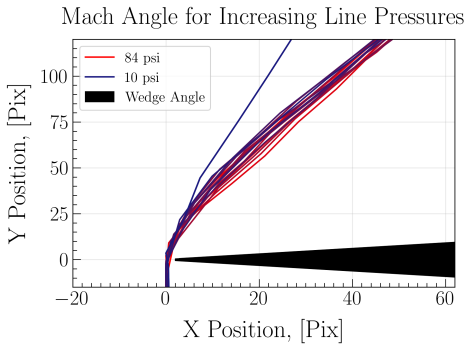

FIG. 4: Line tracing of the shockwaves produced from subjecting a wedge to a high pressure gradient. Colours correspond to increasing tank pressure, from black/blue for low pressure and red for high pressure. Shape and size of wedge has been overlaid for scale.

The traces of the cone shocks can be seen in Fig. 5. Once again, the pressure from the tank is highlighted using a colour gradient where the angle is also not a simply decreasing function of the pressure.

The nature of the shocks for the two samples differed considerably. For the Wedge angle we found that shock waves were produced for applied pressures as low as 10 psi. These shocks got increasingly stronger with increasing pressure, generating shock reflections as can be seen in Fig. 3 for larger psi. The

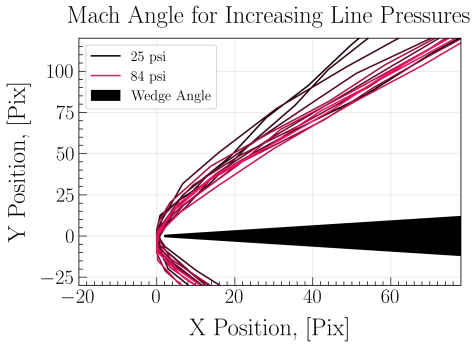

FIG. 5: Line tracing of the shockwaves produced from subjecting a cone to a high pressure gradient. Colours correspond to increasing tank pressure, from black/blue for low pressure and red for high pressure. Shape and size of cone has been overlaid for scale.

shocks were also well-defined in the Schlieren imaging, with fore- and after-shock features also seen in that figure. Of note here is that the upper and lower traces of the shockwave were found to not be symmetric. This is likely due to the machining of the wedge, as there was a slight bevel in the sample.

Conversely, the shocks for the cone were considerably more washed out. This is due, in part to the changes to the Schlieren set-up, but also due to much less well-defined mach angle. This may be due to the fact that the shock was likely a cone itself, lacking an edge that is likely present for the wedge angle.It was also found that the cone only produced a shock wave for pressures larger than 25 psi.

After converting the traces into mach angles for each of the samples and all trials, the mach angles were converted into mach numbers using equation (2). This data can be seen in 6. The lines of best fit were found to be:

$$M(P)_{wedge} = (2.9 \pm 0.6) \cdot 10^{-4} \frac{1}{psi} P + (1.04 \pm 0.003)$$

$$M(P)_{cone} = (1.0 \pm 0.7) \cdot 10^{-4} \frac{1}{psi} P + (1.05 \pm 0.005)$$

The maximum mach number measured for the two samples for the highest possible pressure was also

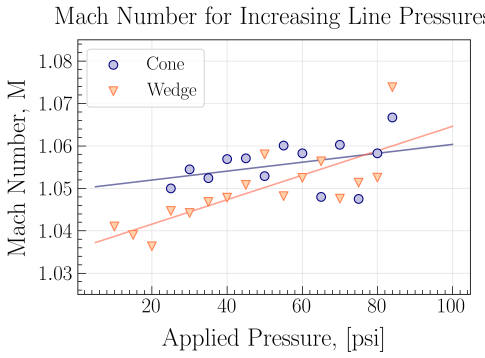

FIG. 6: Calculated Mach number as a function of the applied pressure in the chamber for both the cone and wedge samples. These have been fitted with a simple linear relation with the slopes showing much different behaviour. The cone has a lower slope but nominally higher values while the wedge has a higher slope with lower low pressure mach numbers.

measured to be $M^w_{max} = 1.074$ and $M^c_{max} = 1.066$. Uncertainty for these values was difficult to quantify and will be discussed properly below.

IV. DISCUSSION

In this experiment, two geometrically distinct angled samples with the same impact angle were used a targets for the flow of supersonic air in a high speed wind tunnel. The targets were a wedge of angle $8^0 \pm 0.1$ and a cone with the same angle and length of active region. It was found that the response of the system between the two samples was considerably different. The wedge produced stronger shockwaves up too much lower applied pressures when compared to the cone. This is likely due to the shape of the front of the samples and the ability to dissipate the fluid flow more effectively in the case of the cone.

Determination of the values of the angles in both cases had a significant amount of unaccounted for uncertainty. To begin, when a trial was undertaken, the entire optics table would shake such that the angle of the camera was different in every case. This was mitigated by matching up the wavefronts to a single initial shock point but the asymmetry in the wavefront due about the axis of the sample but this was a difficult process, with the upper and lower shock fronts showing asymmetry due to the angle of the camera. This asymmetry was heightened by the bevel present on the wedge sample and so only the top shock front was analyzed. Another source of uncertainty was due to the tracing of the shock fronts as well as determining the true angle from a curved shock. These uncertainties are somewhat accounted for by the error on the fitting but are not sufficiently accounted for. From Fig. 6, we notice significant spread in the values, and our relations are both not monotonic. The uncertainty on the fitting parameters are supplied and account for this deviation but do not represent the overall systematic uncertainty present.

Of note here is that these calibration fits look quite different between the samples. The cone experiences a much shallower slope but has angles consistent with larger mach numbers for lower pressures than the wedge. Conversely, the wedge has a steeper slope, reaches larger final values and generates shocks for much lower pressures, including the base line pressure. We see that the mach angle behaviour of the samples differs. In addition, as mentioned previously, the qualitative response of the mach angles to pressure gradient input was different as well. The cone produced less defined and powerful shock fronts while less additional features of reflected and after-shocks. This was likely due to the higher flow dissipation efficiency and cone shaped shocks. The difference between the behaviour of the two samples was successfully explored in this experiment.

Further work would include mitigating this and propagating it through the experiment explicitly. Further, the theory of mach angles and shockwaves in supersonic flow is robust and able to describe the scenario in detail better than has been done here, and modelling a cone within the chamber is the next step of this work that was unable to be completed.

V. CONCLUSION

For this lab, the behaviour of shock waves incident to a metal obstruction was investigated for two geometric samples. It was found that the wedge sample produced stronger shock waves as well as better defined shock boundaries and additional reflection shocks not present for the cone. Conversely, imaging the shock produced on the tip of the cone

was much more difficult to resolve, likely due to the increased dissipation efficiency of flow around the cone and the fact that the shock front was likely itself a cone, with worse defined edges. Considerable uncertainty was present in this experiment that made interpreting the results somewhat difficult, but mach numbers were obtained for various applied pressures. The maximum mach number estimated in the chamber at a pressure of 84 psi was found to be $M^w_{max} = 1.074$ and $M^c_{max} = 1.066$. Uncertainties here are likely on the order of 0.01 or greater but were not explicitly found. The mach number function of applied pressure was fitted with linear relations with quite different results for the two samples. These relations are lacking underlying physical theory but adequately serve to calibrate the chamber and demonstrate the increasing mach number in the tube as a function of pressure. These relations were found to be $M(P)_{wedge} = (2.9 \pm 0.6) \cdot 10^{-4} \frac{1}{psi}\ P + (1.04 \pm 0.003)$ for the wedge sample and $M(P)_{cone} = (1.0 \pm 0.7) \cdot 10^{-4} \frac{1}{psi}\ P + (1.05 \pm 0.005)$. Much of the uncertainty present in the problem is then absorbed by the large spread in the data points that make up the fit. The slope of the wedge is significantly larger, while many of the values for the cone are higher. These results show that there exists different behaviour of a shock front depending on the shape of the obstruction and that stronger shock waves are produced for a more oblique surface such as a wedge compared to a cone.

VI. ACKNOWLEDGEMENTS

I would like to thank Dr. Alex Van Netten for machining the sample used here and for aiding in the procedure of this experiment.